String order in dipole-blockaded quantum liquids

String order in dipole-blockaded quantum liquids

Hendrik Weimer

Institut für Theoretische Physik, Leibniz Universität Hannover, Appelstr. 2, 30167 Hannover, Germany

E-mail: hweimer@itp.uni-hannover.de

Abstract

We study the quantum melting of quasi-one-dimensional lattice models in which the dominant energy scale is given by a repulsive dipolar interaction. By constructing an effective low-energy theory, we show that the melting of crystalline phases can occur into two distinct liquid phases having the same algebraic decay of density–density correlations but showing a different non-local correlation function expressing string order. We present possible experimental realizations using ultracold atoms and molecules, introducing an implementation based on resonantly driven Rydberg atoms that offers additional benefits compared to a weak admixture of the Rydberg state.

Keywords: quantum phase transition, dipolar interaction, Rydberg atoms

1. Introduction

The constrained scattering in one-dimensional (1D) quantum systems allows for their effective description in terms of universal low-energy theories even when the microscopic model is not exactly solvable [1]. The most prominent example is the Luttinger liquid, in which all correlation functions decay algebraically according to a single parameter [2]. However, the relation between the actual particles of interest and the low-energy quasiparticles is not always trivial. In this article, we show that for quantum liquids with dominant long-range interactions, the transformation between the two can be highly nonlocal, giving rise to a quantum phase transition between Luttinger liquids differing by string order. Understanding such nonlocal or
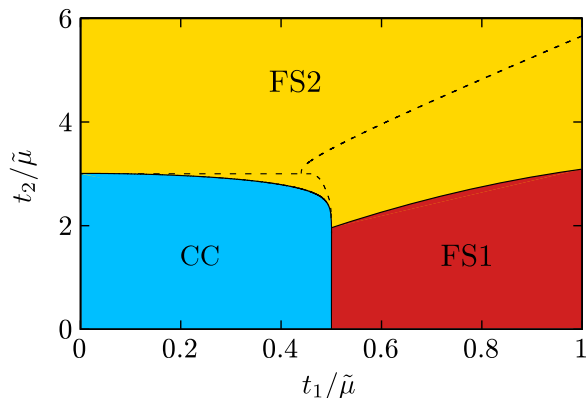
Figure 1. Ground state phase diagram ($U = 4\tilde{\mu}$). Melting of the commensurate crystal (CC) induced by nearest-neighbor hopping t_1 and next-nearest neighbor hopping t_2 result in two distinct floating solid phases (FS1 and FS2) differing by a nonlocal operator characterizing string order. The dashed lines correspond to predictions from a mean-field treatment of the low-energy theory.

topological order is of immense interest as it is key to developing a more general theory of phase transitions beyond the Landau symmetry breaking paradigm [3].

The observation of such exotic phase transitions is often tied to the presence of strong tunable interactions; hence dipolar interactions found within polar molecules [4, 5] or Rydberg atoms [6, 7] serve as ideal candidates and also allow for the combination with well-established tools for studying 1D physics within ultracold quantum gases [8–13]. These recent developments have led to to a wide range of theoretical studies investigating the ground state properties of dipoles in 1D [14–29], giving rise to a plethora of novel many-body phenomena. Of particular interest is the regime of strong repulsive interactions, in which the dipole blockade excludes configurations having two particles in close proximity and leads to strong frustration effects. In the absence of quantum fluctuations, the ground state of a dipole-blockaded lattice gas is characterized by a devil's staircase of gapped crystalline phases commensurate with the underlying lattice [30]. Generically, the quantum fluctuations induced by movement of the particles result in commensurate–incommensurate transitions to a Luttinger liquid [16, 22, 23]. Additional phases can occur pertaining to extended interaction potentials [28] or quasi-1D geometries [25, 29].

In this article, we build on these earlier developments and study dipole-blockaded quantum gases on a triangular ladder. We establish the ground state phase diagram by analyzing an effective low-energy theory describing the dynamics of dislocation defects of the commensurate crystals. Crucially, the melting of the commensurate crystals can be induced by motion either along the direction of the ladder or along its rungs. This leads to the appearance of two distinct floating solid phases (see figure 1), both of which can be described in terms of a Luttinger liquid. Remarkably, we find that the two floating solids cannot be distinguished by merely looking at correlation functions of local operators; instead one has to consider a highly nonlocal observable describing string order. Finally, we comment on possible experimental realizations using ultracold polar molecules or Rydberg atoms, including a novel approach for the latter using laser-induced hopping of Rydberg excitations in an electric field gradient, which can be also used to implement a large class of microscopic models with an unprecedented level of control over hopping and interaction parameters.
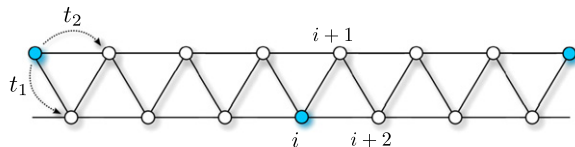
Figure 2. Setup of the system. Dipolar particles are confined to a triangular ladder structure, with hopping occuring along the direction of the ladder (t_2) or along its rungs (t_1). Filled dots indicate the particle positions corresponding to the $q = 7$ commensurate crystal.

2. Hamiltonian description

We start our analysis based on the microscopic Hamiltonian in terms of an extended Hubbard model with long-range dipolar interactions, with the setup of the system depicted in figure 2. In the following, we treat the triangular ladder as a single chain having nearest and next-nearest neighbor hoppings. We point out that the dipole blockade renders the distinction between bosons and fermions irrelevant as the exchange of two particles occurs at very high energy scales, which are unimportant for the low-energy properties of the system. The Hamiltonian is given by

$$H = -t_1 \sum_i \left(c_i c_{i+1}^\dagger + \text{H.c.} \right) - t_2 \sum_i \left(c_i c_{i+2}^\dagger + \text{H.c.} \right)$$
$$+ \sum_{i<j} V_{|i-j|} n_i n_j - \mu \sum_i n_i. \tag{1}$$

Here, t_1 and t_2 are the strength of the nearest and next-nearest neighbor hopping, respectively, $V_{|i-j|}$ accounts for the repulsive dipolar interaction between sites i and j according to the particle number $n_i = c_i^\dagger c_i$, and μ denotes the chemical potential. In the classical limit with $t_1 = t_2 = 0$, the ground state again follows a complete devil's staircase structure of commensurate crystals as the interaction potential is a convex function [30]. The most stable commensurate crystals occur at rational fillings $1/q$ with q being odd, i.e., the particles are located on the two legs of the ladder in an alternating fashion (see figure 2). In the following, we will restrict our analysis to densities close to these values. Here, we are interested in the dipole-blockaded regime with $q \gg 1$, which allows us to approximate many quantities of interest by performing expansions in $1/q$ [21]. For example, the center of the commensurate crystals with filling $1/q$ occurs at a chemical potential of $\mu_0 \approx 32\zeta(3)V_1/q^3$, and the variation in chemical potential over which the phase is stable is given by $\mu_w \approx 168\zeta(5)V_1/q^4$.

3. Effective low-energy theory

We now study the effects of quantum fluctuations induced by t_1 and t_2 within perturbation theory, i.e., $t_1, t_2 \ll \mu$ [16, 21]. The low-energy excitations correspond to dislocation defects of the commensurate crystal, given by the relation $d_j = r_{j+1} - r_j - q$, which measures the deviation of the spacing between the particles j and $j + 1$ from the perfectly commensurate case. Note that these defects are nonlocal quasiparticles, as their position in terms of the original particles depends on the number of defects located at previous sites. Consequently, changing the notation from real particles to defects is a highly nonlocal transformation. To denote this

crucial distinction between lattice sites and defects, we will use the index i when referring to the former and j for the latter. Depending on the sign of d_j, defects occur as hole-like or particle-like, i.e., they decrease or increase the total density, respectively. However, sufficiently far away from the particle-hole symmetric point given by $\mu = \mu_0$, only one of these defects is relevant [21]. Furthermore, the number of defects is a conserved quantity. As the energy cost rapidly increases for $|d_j| > 1$, and the hopping of defects does not exhibit bosonic enhancement, we restrict the Hilbert space to the defect numbers $d_j = 0, 1, 2$. Then the effective low-energy Hamiltonian to first order in t_1, t_2 can be expressed using spin-1 variables as

$$
\begin{aligned}
H = \ & -t_1 \sum_j \left(S_j^+ S_{j+1}^- + \text{H.c} \right) \\
& - t_2 \sum_j \left(S_j^+ S_j^+ S_{j+1}^- S_{j+1}^- + \text{H.c.} \right) \\
& + \tilde{\mu} \sum_j \left(1 + S_j^z \right) + U \sum_j S_j^+ S_j^+ S_j^- S_j^-,
\end{aligned}
\tag{2}
$$

i.e., the next-nearest neighbor hopping t_2 turns into a correlated hopping of the defects. Most importantly, the strong dipolar interaction has been absorbed into the definition of the defects; hence, the resulting low-energy Hamiltonian is purely local and can be further analyzed using standard techniques. In addition to higher order processes in the perturbation series, we also neglect the weak interaction between the defects. The energy cost associated with each defect is given by $\tilde{\mu} = (\mu_0 - \mu + \mu_w/2)/q$, and the repulsion of the defects can be calculated as $U = \mu_w/q$. Note that this model is equivalent to a Bose–Hubbard model with correlated hopping and a three-body constraint [31].

If one of the hopping terms vanishes, the phase boundaries can be determined exactly by mapping the problem onto free fermions [32]. For $t_2 = 0$, the on-site repulsion U is irrelevant at the phase transition, which occurs at $t_1 = \tilde{\mu}/2$ between the $n = 0$ Mott insulator and a liquid phase with finite defect density. Likewise, there is a second phase transition for $t_1 = 0$ occuring at $t_2 = \tilde{\mu} + U/2$. Remarkably, this second liquid has defects that always appear in pairs as the single-defect sector is still protected by a gap of $\tilde{\mu}$. In the following, we refer to the latter phase as a 'pair defect liquid,' while calling the former a 'single defect liquid.' Based on the low-energy Hamiltonian, equation (2), we map out the complete phase diagram using mean-field theory and an exact density-matrix renormalization group (DMRG) method based on a matrix-product state approach [33, 34]; see figure 1. The transition line between the two liquid phases corresponds to the decay of the spin correlation function $\langle S_j^+ S_k^- \rangle$ changing from algebraic to exponential behavior, as shown in figure 3. Here, we determine the transition line from the comparison of an algebraic and an exponential fit to the correlation function for a system of 30 spins. As noted previously [31], mean-field theory produces good qualitative agreement with the DMRG results, and furthermore yields the correct values for the transition in the exactly solvable cases.

In order to understand the transition between the two liquid phases in more detail, it is instructive to represent the effective spin-1 model by two spin-1/2 degrees of freedom, which then can be bosonized [35]. Then, sufficiently far away from the transition, we know from the free fermion solution that the system is well described in terms of a single component Luttinger liquid, i.e., the second bosonic field is massive, according to the effective Hamiltonian
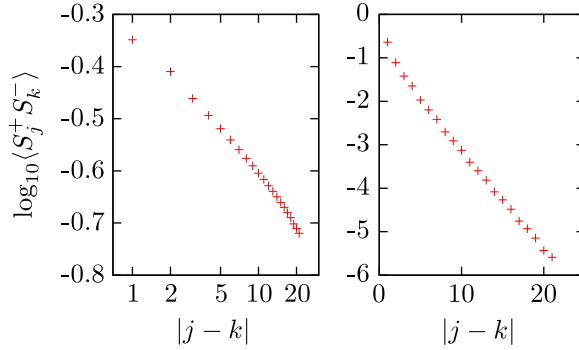
Figure 3. Decay of spin correlations in the low-energy theory for a system of 30 spins ($U = 4\tilde{\mu}$, $t_1 = 0.6\tilde{\mu}$). Upon increasing the pair hopping t_2, the system undergoes a phase transition from an atomic defect liquid with an algebraic decay ($t_2 = 1.5\tilde{\mu}$, left) to a pair defect liquid showing an exponential decay ($t_2 = 3.0\tilde{\mu}$, right).

$$H = \frac{v_j}{2\pi} \int \mathrm{d}x \left[K_j \left(\pi \Pi_j(x) \right)^2 + \frac{1}{K_j} \left(\nabla \phi_j(x) \right)^2 \right], \tag{3}$$

where Π_j and $\nabla \phi_j$ are bosonic fields corresponding to phase and density fluctuations. If the fields with $j = 1$ are gapless, then the system is in the single defect liquid phase, while gapless $j = 2$ fields correspond to the pair defect liquid. In the limit of low defect densities, we find $K_j = K = 1$ for the Luttinger parameter, while the speed of sound is given by $v_1 = qa\sqrt{\tilde{\mu}t_1/2}$ and $v_2 = qa\sqrt{(2\tilde{\mu} + U)t_2/2}$, respectively. The transition between the single and the double defect liquid is of the Ising universality class [36–38]. From the finite-size scaling behavior of the underlying Ising transition [39], we can estimate the error in determining the phase boundary between the two liquid phases in our DMRG calculation to behave as $\sim 1/\tilde{L}^2$, with $\tilde{L}$ being the number of bulk spins considered in the fitting procedure. Here, we have used a value of $\tilde{L} = 18$, corresponding to an error from the finiteness of the system of about 1 percent.

4. String order

Within the validity of our perturbative approach, the phase boundaries of the defect model (2) corresponds to the phase boundaries of the microscopic Hamiltonian (1). However, we are rather interested in describing the appearing quantum phases in terms of observables involving the microscopic degrees of freedom, i.e., correlations between individual particles rather than correlations between the defects. In the following, we apply Luttinger liquid theory to classify the ground state phases in terms of the microscopic particles.

When mapping from the defect description to the real particles, we first note that the $n = 0$ Mott insulator for the defects corresponds to the commensurate crystal at filling $1/q$, in which the density–density correlation $\langle n_{iq} n_0 \rangle$ exhibits true long-range order. In the two liquid phases, we find the density–density correlations of the microscopic particles to asymptotically decay as $\langle n_x n_0 \rangle \sim x^{-2K/(n_d+q)^2}$, where n_d is the density of the defects [21]. Consequently, while the existence of algebraically decaying correlations signals the melting of the commensurate crystal phase, it is not possible to distinguish the two defect liquids. Thus, explaining the phase diagram in terms of the microscopic particles requires the probing of nonlocal correlations.

However, we already know that the single defect correlation $\langle (1 - S_z^2)^{(0)}(1 - S_z^2)^{(j)} \rangle$ exhibits an algebraic decay in the single defect liquid and an exponential decay in the pair defect liquid. Remarkably, here we find that this behavior can be captured in terms of the microscopic variables by introducing an observable measuring string order,

$$O_{\text{string}}(x) = \left\langle \exp\left(i2\pi/q \sum_{k=0}^{x} n_k n_{k+q-1} \right) \right\rangle. \tag{4}$$

Here, we have focused on the case of particle-like defects; an analogous expression for hole-like defects follows by replacing n_{k+q-1} by n_{k+q+1}. Most importantly, the term inside the exponential is proportional to the number of single defects N_x occuring over a distance x. Then the value of $O_{\text{string}}(x)$ simply follows from the characteristic function of the probability distribution of N_x. In the pair defect liquid phase, the single defects are uncorrelated, meaning N_x satisfies a Poisson distribution with a mean growing linearly with x. Consequently, $O_{\text{string}}(x)$ decays exponentially with distance in the pair liquid phase. In the single defect liquid, however, N_x is given by a discrete Gaussian distribution whose mean also grows linearly with x but having a variance $\sigma^2 = K \log(x/b)/\pi^2$, where b is a short distance cutoff [21]. From its characteristic function, we identify the leading term in the long distance limit decaying according to an algebraic function, $O_{\text{string}}(x) \sim x^{-2 K/q^2}$.

   As the slowest decaying correlation function is still given by the microscopic density–density correlations, both phases form a 'floating solid' on top of the underlying lattice. We denote them by FS1 and FS2, respectively, with the former corresponding to the single defect liquid and thus exhibiting an algebraic decay of the string correlations. Note that in contrast to the phases exhibiting string order known as Haldane insulators [14, 40, 41], both floating solid phases are gapless. The full phase diagram is shown in figure 1.

5. Experimental realization

Let us now turn to possible experimental implementations of the extended Hubbard model introduced in equation (1). In any of the setups discussed in the following, the triangular lattice structure is created using standard optical lattice beams [42]. Additionally, string order can be measured by direct imaging of atoms or molecules in the lattice [12, 13].

5.1. Ultracold polar molecules

As a first possible implementation, we consider a setup based on ultracold polar molecules [4, 5]. Here, the molecules are prepared in the rovibrational ground state and loaded into the triangular lattice. The hopping matrix elements t_1 and t_2 follow from the tunneling of the molecules in the lattice potential. The repulsive dipole–dipole interaction V_{ij} can be realized either by applying a strong electric field [43] or by microwave dressing of the rotational excitations [44, 45]. For LiCs molecules having an electric dipole moment of $d = 5.5$ D, the characteristic energy scale $\tilde{\mu}$ close to the $q = 7$ commensurate crystal on a $a = 532$ nm lattice is given by $\tilde{\mu} \approx 2\pi\hbar \times 100$ Hz, which is compatible with experimental timescales within these systems.
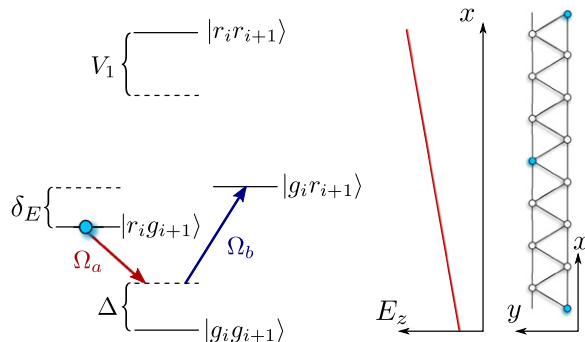
Figure 4. Energy levels of two adjacent atoms for laser-induced hopping of Rydberg excitations in an electric field gradient. The detuning between two Rydberg excitation lasers compensates the differential Stark shift $\delta_E = d\,(E_z^{(i+1)} - E_z^{(i)})$ created by the field gradient, while the $|r_i r_{i+1}\rangle$ state becomes far detuned through the dipolar interaction V_1.

5.2. Rydberg atoms

Alternatively, our model can also be realized using ultracold Rydberg atoms [6, 7]. A straightforward implementation would consist of a weak coupling Ω to a Rydberg state detuned by Δ_r [46–48], where the strong repulsive interactions between Rydberg states create an interaction potential asymptotically decaying as $1/x^3$ for Rydberg states within the Stark fan. However, the experimental parameters for such a Rydberg dressing are quite challenging: in particular, the dipolar interaction is suppressed by a factor $\sim(\Omega/\Delta_r)^4$, while the radiative decay limiting the lifetime of the system only decreases as $(\Omega/\Delta_r)^2$. Therefore, we present here a different route benefitting from resonant excitations to the Rydberg state. Initially, the atoms are loaded into a deep optical lattice, forming a Mott insulator state with one atom per lattice site. Then, the extended Hubbard model defined in equation (1) is realized by treating atoms in their electronic ground state $|g\rangle$ as empty sites and atoms in a Rydberg state $|r\rangle$ as particles. Here, a finite density of Rydberg excitations is created by adiabatically tuning the excitation lasers [49–51], which will control the value of the chemical potential μ. Finally, an electric field gradient is introduced, such that the difference in the Stark shift between different sites is exactly canceled by the detuning between two excitation lasers (see figure 4), resulting in a hopping of the Rydberg excitations. Note that this process crucially relies on the dipole blockade between neighboring sites; for noninteracting particles the two paths via $|g_i g_{i+1}\rangle$ and $|r_i r_{i+1}\rangle$ interfere destructively. By introducing an additional laser, it is possible to satisfy this resonance condition for both nearest-neighbor and next-nearest-neighbor distances. The coupling constants t_1 and t_2 derived from the induced hoppings of the Rydberg excitations $\sim\Omega_a \Omega_b / 2\Delta$ can be controlled independently by the intensities of the excitation lasers. Here, we find that for a Rydberg state with a principal quantum number of $n = 43$ in an $a = 1\ \mu$m lattice, the liquid phases close to the $q = 7$ commensurate crystal form around a characteristic energy scale of $\tilde{\mu} \approx 2\pi\hbar \times 400$ kHz, which is several orders of magnitude larger than the decay rate of the Rydberg state. We would like to stress that this implementation procedure based on electric field gradients is quite general and can readily be extended to a large class of extended Hubbard models with tunable long-range hoppings and interactions.

6. Conclusions

In summary, we have shown that dipole-blockaded quantum gases on triangular ladders support two distinct liquid phases, differing by string order. While the identical behavior of local correlation functions would suggest that both liquids share an effective low-energy description in terms of the same Luttinger liquid, the different nature of the quasiparticle excitations defies this intuition. Our interpretation in terms of nonlocal quasiparticle excitations could also lead to a better understanding of related models with long-range interactions [25, 28].

Acknowledgements

References

[1] Giamarchi T 2004 *Quantum Physics in One Dimension* (Oxford: Clarendon)
[2] Haldane F D M 1981 *Phys. Rev. Lett.* **47** 1840
[3] Wen X-G 2013 *ISRN Cond. Mat. Phys.* **16** 20
[4] Carr L D and Ye J 2009 *New J. Phys.* **11** 055009
[5] Baranov M A, Dalmonte M, Pupillo G and Zoller P 2012 *Chem. Rev.* **112** 5012
[6] Saffman M, Walker T G and Mølmer K 2010 *Rev. Mod. Phys.* **82** 2313
[7] Löw R, Weimer H, Nipper J, Balewski J B, Butscher B, Büchler H P and Pfau T 2012 *J. Phys.* B **45** 113001
[8] Paredes B, Widera A, Murg V, Mandel O, Fölling S, Cirac I, Shlyapnikov G V, Hänsch T W and Bloch I 2004 *Nature* **429** 277
[9] Kinoshita T, Wenger T and Weiss D S 2004 *Science* **305** 1125
[10] Syassen N, Bauer D M, Lettner M, Volz T, Dietze D, García-Ripoll J J, Cirac J I, Rempe G and Dürr S 2008 *Science* **320** 1329
[11] Haller E, Hart R, Mark M J, Danzl J G, Reichsöllner L, Gustavsson M, Dalmonte M, Pupillo G and Nägerl H-C 2010 *Nature* **466** 597
[12] Simon J, Bakr W S, Ma R, Tai M E, Preiss P M and Greiner M 2011 *Nature* **472** 307
[13] Endres M *et al* 2011 *Science* **334** 200
[14] Dalla Torre E G, Berg E and Altman E 2006 *Phys. Rev. Lett.* **97** 260401
[15] Kollath C, Meyer J S and Giamarchi T 2008 *Phys. Rev. Lett.* **100** 130403
[16] Burnell F J, Parish M M, Cooper N R and Sondhi S L 2009 *Phys. Rev.* B **80** 174519
[17] Schachenmayer J, Lesanovsky I, Micheli A and Daley A J 2010 *New J. Phys* **12** 103044
[18] Hauke P, Cucchietti F M, Müller-Hermes A, Bañuls M-C, Cirac J I and Lewenstein M 2010 *New J. Phys.* **12** 113037
[19] Pikovski A, Klawunn M, Shlyapnikov G V and Santos L 2010 *Phys. Rev. Lett.* **105** 215302
[20] Dalmonte M, Pupillo G and Zoller P 2010 *Phys. Rev. Lett.* **105** 140401
[21] Weimer H and Büchler H P 2010 *Phys. Rev. Lett.* **105** 230403
[22] Sela E, Punk M and Garst M 2011 *Phys. Rev.* B **84** 085434
[23] Lauer A, Muth D and Fleischhauer M 2012 *New J. Phys.* **14** 095009
[24] Ruhman J, Dalla Torre E G, Huber S D and Altman E 2012 *Phys. Rev.* B **85** 125121
[25] Bauer M and Parish M M 2012 *Phys. Rev. Lett.* **108** 255302
[26] Knap M, Berg E, Ganahl M and Demler E 2012 *Phys. Rev.* B **86** 064501

[27] Manmana S R, Stoudenmire E M, Hazzard K R A, Rey A M and Gorshkov A V 2013 *Phys. Rev. B* **87** 081106
[28] Mattioli M, Dalmonte M, Lechner W and Pupillo G 2013 *Phys. Rev. Lett.* **111** 165302
[29] Gammelmark S and Zinner N T 2013 *Phys. Rev. B* **88** 245135
[30] Bak P and Bruinsma R 1982 *Phys. Rev. Lett.* **49** 249
[31] Mazza L, Rizzi M, Lewenstein M and Cirac J I 2010 *Phys. Rev. A* **82** 043629
[32] Sachdev S 1999 *Quantum Phase Transitions* (Cambridge: Cambridge University Press)
[33] M L Wall and the Carr Theoretical Physics Research Group 2014 'Open Source MPS', https://sourceforge.net/p/openmps/, (software, v1.0, 2014)
[34] Wall M L and Carr L D 2012 *New J. Phys.* **14** 125015
[35] Timonen J and Luther A 1985 *J. Phys. C* **18** 1439
[36] Romans M W J, Duine R A, Sachdev S and Stoof H T C 2004 *Phys. Rev. Lett.* **93** 020405
[37] Manmana S R, Läuchli A M, Essler F H L and Mila F 2011 *Phys. Rev. B* **83** 184433
[38] Ejima S, Bhaseen M J, Hohenadler M, Essler F H L, Fehske H and Simons B D 2011 *Phys. Rev. Lett.* **106** 015303
[39] Burkhardt T W and Guim I 1985 *J. Phys. A* **18** L33
[40] den Nijs M and Rommelse K 1989 *Phys. Rev. B* **40** 4709
[41] Kennedy T and Tasaki H 1992 *Phys. Rev. B* **45** 304
[42] Bloch I, Dalibard J and Zwerger W 2008 *Rev. Mod. Phys.* **80** 885
[43] Büchler H P, Demler E, Lukin M, Micheli A, Prokof'ev N, Pupillo G and Zoller P 2007 *Phys. Rev. Lett.* **98** 060404
[44] Lemeshko M, Krems R V and Weimer H 2012 *Phys. Rev. Lett.* **109** 035301
[45] Yan B, Moses S A, Gadway B, Covey J P, Hazzard K R A, Rey A M, Jin D S and Ye J 2013 *Nature* **501** 521
[46] Henkel N, Nath R and Pohl T 2010 *Phys. Rev. Lett.* **104** 195302
[47] Pupillo G, Micheli A, Boninsegni M, Lesanovsky I and Zoller P 2010 *Phys. Rev. Lett.* **104** 223002
[48] Honer J, Weimer H, Pfau T and Büchler H P 2010 *Phys. Rev. Lett.* **105** 160404
[49] Pohl T, Demler E and Lukin M D 2010 *Phys. Rev. Lett.* **104** 043002
[50] van Bijnen R M W, Smit S, van Leeuwen K A H, Vredenbregt E J D and Kokkelmans S J J M F 2011 *J. Phys. B* **44** 184008
[51] Weimer H, Yao N Y, Laumann C R and Lukin M D 2012 *Phys. Rev. Lett.* **108** 100501